RENEB Inter-Laboratory Comparison 2021: The Gene Expression Assay

Authors: Abend, M., Amundson, S.A., Badie, C., Brzoska, K., Kriehuber, R., et al.

Source: Radiation Research, 199(6) : 598-615

Published By: Radiation Research Society

URL: https://doi.org/10.1667/RADE-22-00206.1

RADIATION RESEARCH **199**, 598–615 (2023)
0033-7587/23 $15.00

DOI: 10.1667/RADE-22-00206.1

RENEB Inter-Laboratory Comparison 2021: The Gene Expression Assay

M. Abend,[a,1] S.A. Amundson,[b] C. Badie,[c] K. Brzoska,[d] R. Kriehuber,[e] J. Lacombe,[f] M. Lopez-Riego,[g] K. Lumniczky,[h] D. Endesfelder,[i] G. O'Brien,[c] S. Doucha-Senf,[a] S.A. Ghandhi,[b] R. Hargitai,[h] E. Kis,[h] L. Lundholm,[g] D. Oskamp,[e] P. Ostheim,[a] S. Schüle,[a] D. Schwanke,[a] I. Shuryak,[b] C. Siebenwith,[a] M. Unverricht-Yeboah,[e] A. Wojcik,[g] J. Yang,[f] F. Zenhausern,[f] M. Port[a]

[a]Bundeswehr Institute of Radiobiology, Munich, Germany; [b]Columbia University Irving Medical Center, Center for Radiological Research, New York, New York: [c]UK Health Security Agency and Office for Health Improvement and Disparities, Centre for Radiation, Chemical and Environmental Hazards, Oxfordshire, England; [d]Institute of Nuclear Chemistry and Technology, Centre for Radiobiology and Biological Dosimetry, Warsaw, Poland; [e]Forschungszentrum Jülich, Department of Safety and Radiation Protection, Jülich, Germany [f]University of Arizona, Center for Applied Nanobioscience & Medicine, Phoenix, Arizona: [g]Department of Molecular Biosciences, The Wenner-Gren Institute, Stockholm University, Stockholm, Sweden; [h]Radiation Medicine Unit, Department of Radiobiology and Radiohygiene, National Public Health Centre, Budapest, Hungary; [i]Bundesamt für Strahlenschutz, BfS, Oberschleißheim, Germany

Abend M, Amundson SA, Badie C, Brzoska K, Kriehuber R, Lacombe J, Lopez-Riego M, Lumniczky K, Endesfelder D, O'Brien G, Doucha-Senf S, Ghandhi SA, Hargitai R, Kis E, Lundholm L, Oskamp D, Ostheim P, Schüle S, Schwanke D, Shuryak I, Siebenwith C, Unverricht-Yeboah M, Wojcik A, Yang J, Zenhausern F, Port M. RENEB Inter-Laboratory Comparison 2021: The Gene Expression Assay. Radiat Res. 199, 598–615 (2023).

Early and high-throughput individual dose estimates are essential following large-scale radiation exposure events. In the context of the Running the European Network for Biodosimetry and Physical Dosimetry (RENEB) 2021 exercise, gene expression assays were conducted and their corresponding performance for dose-assessment is presented in this publication. Three blinded, coded whole blood samples from healthy donors were exposed to 0, 1.2 and 3.5 Gy X-ray doses (240 kVp, 1 Gy/min) using the X-ray source Yxlon. These exposures correspond to clinically relevant groups of unexposed, low dose (no severe acute health effects expected) and high dose exposed individuals (requiring early intensive medical health care). Samples were sent to eight teams for dose estimation and identification of clinically relevant groups. For quantitative reverse transcription polymerase chain reaction (qRT-PCR) and microarray analyses, samples were lysed, stored at 20°C and shipped on wet ice. RNA isolations and assays were run in each laboratory according to locally established protocols. The time-to-result for both rough early and more precise later reports has been documented where possible. Accuracy of dose estimates was calculated as the difference between estimated and reference doses for all doses (summed absolute difference, SAD) and by determining the number of correctly reported dose estimates that were defined as ±0.5 Gy for reference doses <2.5 Gy and ±1.0 Gy for reference doses >3 Gy, as recommended for triage dosimetry. We also examined the allocation of dose estimates to clinically/diagnostically relevant exposure groups. Altogether, 105 dose estimates were reported by the eight teams, and the earliest report times on dose categories and estimates were 5 h and 9 h, respectively. The coefficient of variation for 85% of all 436 qRT-PCR measurements did not exceed 10%. One team reported dose estimates that systematically deviated several-fold from reported dose estimates, and these outliers were excluded from further analysis. Teams employing a combination of several genes generated about two-times lower median SADs (0.8 Gy) compared to dose estimates based on single genes only (1.7 Gy). When considering the uncertainty intervals for triage dosimetry, dose estimates of all teams together were correctly reported in 100% of the 0 Gy, 50% of the 1.2 Gy and 50% of the 3.5 Gy exposed samples. The order of dose estimates (from lowest to highest) corresponding to three dose categories (unexposed, low dose and highest exposure) were correctly reported by all teams and all chosen genes or gene combinations. Furthermore, if teams reported no exposure or an exposure >3.5 Gy, it was always correctly allocated to the unexposed and the highly exposed group, while low exposed (1.2 Gy) samples sometimes could not be discriminated from highly (3.5 Gy) exposed samples. All teams used *FDXR* and 78.1% of correct dose estimates used *FDXR* as one of the predictors. Still, the accuracy of reported dose estimates based on *FDXR* differed considerably among teams with one team's SAD (0.5 Gy) being comparable to the dose accuracy employing a combination of genes. Using the workflow of this reference team, we performed additional experiments after the exercise on residual RNA and cDNA sent by six teams to the reference team. All samples were processed similarly with the intention to improve the accuracy of dose estimates when employing the same workflow. Re-evaluated dose estimates improved for half of the samples and worsened for the others. In conclusion, this inter-laboratory comparison exercise enabled (*1*) identification of technical problems and corrections in preparations for future events, (*2*) confirmed the early and high-throughput capabilities of gene expression, (*3*) emphasized different biodosimetry approaches using either only *FDXR* or a gene combination, (*4*) indicated some

[1] Corresponding author: Michael Abend, M.D., Bundeswehr Institute of Radiobiology affiliated to University Ulm, Neuherbergstr. 11, 80937 Munich, Germany; email: michaelabend@bundeswehr.org.

improvements in dose estimation with *FDXR* when employing a similar methodology, which requires further research for the final conclusion and (*5*) underlined the applicability of gene expression for identification of unexposed and highly exposed samples, supporting medical management in radiological or nuclear scenarios.

INTRODUCTION

Potential large-scale radiological mass casualties require preparedness for determining individual doses. At regular intervals, Running the European Network for Biodosimetry and Physical Dosimetry (RENEB) performs inter-laboratory comparison (ILC) exercises using ex vivo-irradiated blinded, coded samples to validate assay performance and laboratories for individual biodosimetry purposes (*1–11*). The RENEB ILC 2021 is presented in this issue as a series of manuscripts. The introductory inter-assay comparison article is followed by separate articles dedicated to results for each assay. This manuscript focuses on the gene expression results only.

Early and high-throughput assessment of exposed individuals would be required to evaluate the extent of radiation injuries as quickly as possible and, when needed, initiate appropriate treatment (*12*). In the absence of physical dosimeters (e.g., in case of terrorist attacks when badge dosimeters are not routinely worn by those likely to be exposed), biological changes after radiation exposure can be used to estimate individual doses. The gold standard in the field of biological dosimetry is scoring dicentric chromosomes. The method is specific for ionizing radiation, sensitive, very reliable, but time-consuming (*13, 14*). The expression of several genes (e.g., related to the p53 signal transduction pathway) has already been shown to be modulated in a dose-dependent manner (*15, 16*) and there is strong evidence for gene expression to be used as a complementary tool for early (*17, 18*) and high-throughput minimally invasive individual radiation biodosimetry (*19–24*).

Here, gene expression analyses of candidate genes were performed in eight independent laboratories using different technologies, namely quantitative reverse transcription polymerase chain reaction (qRT-PCR, seven teams) and a microarray platform (one team) and different analysis protocols. We asked for early reports of dose estimates to examine the method's speed given optimal conditions and running the assay with high priority. Reported dose estimates were compared by calculating the difference between estimated and reference doses among teams. Results within ± 0.5 Gy or ± 1.0 Gy for reference doses <2.5 Gy or >3 Gy, respectively, were classified as successful, as recommended for triage dosimetry (25). The reference doses of unexposed, low exposed (1.2 Gy), and high exposed (3.5 Gy) samples correspond to clinically relevant dose categories of unexposed, low dose (no severe acute health effects expected) and high dose exposed individuals (requiring early intensive medical health care). We calculated the allocation of reported dose estimates to these clinically relevant groups. Teams used either one gene or a combination of genes. In particular the well-known radiation-response gene *FDXR* was used by all teams. In a final step after the exercise, we performed additional tests to elucidate whether a similar workflow and data analysis might increase the accuracy of dose estimates based on *FDXR* gene expression changes.

MATERIALS AND METHODS

Procedures Common for All Assays

Blood sampling in heparinized vials (2–3 ml whole blood was provided from one healthy 30-year-old female donor for calibration samples and one healthy 32-year-old male donor for blinded, coded

TABLE 1
Overview of Participating Teams, Utilized Platforms, Number and Names of Genes or Gene Combinations Used, the Origin of Calibration Samples, and Further Details

Team ID	Platform	No. genes	Gene name	Housekeeping genes	Samples used and further specifications
1	qRT-PCR	2	GDF15, FDXR	UBC	blinded coded and calibration samples from BIR
2	qRT-PCR	8	BAX, BBC3, CDKN1A, DDB2, FDXR, GADD45A, GDF15, TNFSF4	ITFG1, DPM1	blinded coded and calibration samples from BIR. Additional calibration samples were generated at team 2
3	qRT-PCR	3	CDKN1A, DDB2, FDXR	MRPS5	blinded coded and calibration samples from BIR
4	qRT-PCR	4	GADD45A, FDXR, CDKN1A, MDM2	18S rRNA	blinded coded and calibration samples from BIR. Additional calibration samples from one donor collected at two different time points were generated at team 4
5	qRT-PCR	3	FDXR, DDB2, CDKN1A	HPRT, ITFG1, GAPDH	blinded coded and calibration samples from BIR, samples were processed by 2 experts
6	qRT-PCR	1	FDXR	HPRT	blinded coded and calibration samples from BIR
7	qRT-PCR	2	FDXR, DDB2	18S rRNA	blinded coded and calibration samples from BIR
8	Microarrays	4 resp. 1	TNFSF4, FDXR, PHLDA3, THC2705989, resp. FDXR	GAPDH	blinded coded samples only

TABLE 2
Overview of Methodological Details of Either qRT-PCR (Quantitative Reverse Transcription Polymerase Chain Reaction) or Microarrays Used by the Contributing Teams

qRT-PCR workflow	qRT-PCR 1	qRT-PCR 2	qRT-PCR 3	qRT-PCR 4
RNA isolation				
Isolation kit	QIAamp RNA Blood Mini Kit	QIAamp RNA Blood Mini Kit	QIAamp RNA Blood Mini Kit	Red blood cell lysis buffer, Roche E.Z.N.A. Total RNA Kit I, Omega BIO-TEK
DNA digestion during isolation	RNase-free DNase-Set (Qiagen)	RNase-free DNase-Set (Qiagen)	RNase-free DNase-Set (Qiagen)	No
Template eluted in:	RNAse-free water	RNAse-free water	RNAse-free water	RNAse-free water
Quality control				
RNA integrity number	No	No	Yes	No
RNA concentration	Yes (NanoDrop™)	Yes (Quantus™ Fluorometer, Promega)	Yes (BioTek Epoch)	Yes (NanoDrop™)
A260/280	Yes	No	Yes	Yes
A260/230	Yes	No	No	Yes
Check DNA conta mination		No	No	No - FDXR, MDM2 and CDKN1A primer sequences designed to span exon-exon boundaries. 18S sequence described below. Additionally, all column RNA prep kits remove most of the DNA.
cDNA synthesis				
Kit/MasterMix	High Capacity cDNA Reverse Transcription Kit (Thermo Fisher Scientific)	High Capacity cDNA Reverse Transcription Kit (Thermo Fisher Scientific)	QuantiTect Reverse Transcription (Qiagen)	High Capacity cDNA Reverse Transcription Kit (Thermo Fisher Scientific)
PCR protocol	1×/25°C/10min, 1×/37°C/ 120min, 1×/85°C/5min	1×/25°C/10min, 1×/37°C/ 120min, 1×/85°C/5min	1×/42°C/2min, ice 1×/42°C/20min, 1×/95°C/3min	1×/25°C/10min, 1×/37°C/120min, 1×/85°C/5min
Quality control	UBC Ct	ITFG1 Ct, DPM1 Ct	MRPS5 Ct	No
qRT-PCR				
Kit/MasterMix	TaqMan Universal Master Mix	TaqMan Universal Master Mix II, no UNG (Thermo Fisher Scientific)	QuantiFast SYBR Green PCR (Qiagen)	5× HOT FIREPol® EvaGreen® qPCR SuperMix, Solis BioDyne
TaqMan assays SYBR Green assay	FDXR (Hs00244586_m1), GDF15 (Hs00171132_m1)	BAX (Hs00180269_m1), BBC3 (Hs00248075_m1), CDKN1A (Hs00355782_m1), DDB2 (Hs03044953_m1), FDXR (Hs00244586_m1), GADD45A (Hs00169255_m1), GDF15 (Hs00171132_m1), TNFSF4 (Hs00182411_m1)	CDKN1A-F: AGACCAGCATGACAGATTTCTACC; CDKN1A-R: CTTCCTGTGGGCGGATTAGG; DDB2-F: AGCATCACTGGGCTGAAGTT; DDB2-R: TGGTGTCTGAGCTGGCAAAA; FDX-F: TGGAGAGAACGGACATCACG; FDX-R: AGCCACACTGTCTTCACTCG	GADD45a for: ACTGCGTGCTGGTGACGAAT, GADD45a rev: GTTGACTTAAGGCAGGATCCTTCCA; FDXR for: TGGATGTGCCAGGCCTCTAC, FDXR rev: TGAGGAAGCTGTCAGTCATGGTT; CDKN1A for: CCTGGAGACTCTCAGGGTCGAAA, CDKN1A rev: GCGTTTGGAGTGGTAGAAATCTGTCA; MDM2 for: TATCAGGCAGGGGAGAGTGATACA, MDM2 rev: CCAACATCTGTTGCAATGTGATGGAA; 18S for: GCTTAATTTGACTCAACACGGGA, 18S rev: AGCTATCAATCTGTCAATCCTGTCC.
Cycles	1×/50°C/2min, 95°C/ 10min, 40×/95°C/15 s, 60°C/1min	1×/95°C/10min, 40×/ 95°C/15 s, 60°C/1min	1×/95°C/5min, 40×/95°C/10 s, 60°C/30s	1×/95°C/15min, 45×/95°C/15s, 60°C/20s, 72°C/20s, 1×/95°C/5s, 1×/65°C/60s, 1×/97°C, cooling step
Detection system	QS7 Flex (Thermofisher)	7500 Real-Time PCR System (Thermo Fischer Scientific)	Stratagene Mx30005P (Agilent Technologies, Inc.)	LightCycler® 480 Instrument, Roche
Threshold	0.15		fixed	Second Derivative Maximum method
Normalization	UBC (Hs00824723_m1)	ΔCt(target gene) = Ct(target gene) - √(Ct(ITFG1) ×Ct(DPM1)) ITFG1 (Hs00229263_m1), DPM1 (Hs00187270_m1)	MRPS5-F: TAAACGGGAGCGAGGATGGA; MRPS5-R: ATGTTTCTCCACAGGGACCAG	Human 18S rRNA (sequence, forward: GCTTAATTTGACTCAACACGGGA, reverse: AGCTATCAATCTGTCAATCCTGTCC, Thermo Fisher Scientific)
Quantification method	Δ-Ct approach	Δ-Ct approach	ΔΔ-Ct approach, relative fold change in relation to the 0 Gy sample of the calibration curve	Δ-Ct approach
Quality control				
Standard curve	No	No	Yes	No
Slope	No	No	No	No
r-sqr	No	No	Yes	No
18s rRNA Cq	UBC	ITFG1, DPM1	MRPS5	Yes

Note. The sequence of topics from top to bottom reflects a typical workflow for gene expression analysis, starting with RNA-isolation, quality and quantity controls, cDNA synthesis and qRT-PCR.

TABLE 2
Extended.

qRT-PCR			Microarrays	
5	6	7	Microarray workflow	Microarrays 8
			RNA isolation	
QIAamp RNA Blood Mini Kit	QIAamp RNA Blood Mini Kit	QIAamp RNA Blood Mini Kit	Isolation kit	QIAamp RNA Blood Mini Kit
RNase-free DNase-Set (Qiagen)	RNase-free DNase-Set (Qiagen)	RNase-free DNase-Set (Qiagen)	DNA digestion during isolation	RNase-free DNase-Set (Qiagen)
RNAse-free water	RNAse-free water	RNAse-free water	Template eluted in:	RNAse-free water
			Quality control	
Yes; for calibration samples: RIN>9.1; for blinded samples: RIN>8.0	Yes	Yes	RNA integrity number	Yes
Yes (Take3 micro-volume plate, Synergy HT, Biotek)	Yes (NanoDrop™)	Yes (NanoDrop™)	RNA concentration	Yes (NanoDrop™)
Yes	Yes	Yes	A260/280	Yes
Yes	Yes	Yes	A260/230	Yes
(-) RT control		conventional PCR (ß-actin primer, HotStar MasterMix (Qiagen), 30 cycles)	Check DNA conta mination	No
			cDNA synthesis	
RevertAid First Strand cDNA Synthesis Kit (Thermo Scientific)	High Capacity cDNA Archive Kit	High Capacity cDNA Reverse Transcription Kit (Thermo Fisher Scientific)	Kit/MasterMix	Quick Amp Labeling Kit (Agilent)
1×/25°C/5min, 1×/42°C/60min, 1×/70°C/5min	1×/25°C/10min, 1×/37°C/ 120min, 1×/85°C/5min	1×/25°C/10min, 1×/37°C/120min	PCR protocol	1×/40°C/120min, 1×/70°C/ 15min; 1×/40°C/120min
	HPRT1 Ct	18S rRNA Ct	Quality control	NanoDrop ™
			Microarray	
TaqMan fast advanced master mix (Applied Biosystems) and Maxima SYBR Green qPCR Master Mix (Thermo Scientific)	TaqMan,PerfeCTa®, MultiPlex qPCR SuperMix, Quanta bioscience	TaqMan Universal Master Mix	DNA-Microarray	Agilent, 44k whole human genome, G4112F
TaqMan® assay: DDB2 (Hs00172068_m1), FDXR (HS01031617_m1), ITFG1: Hs01061271_m1 SYBR Green assay: CDKN1A F:CCT CAT CCC GTG TTC TCC TTT CDKN1A R: GTA CCA CCC AGC GGA CAA GT GAPDH F: CGA CCA CTT TGT CAA GCT CA GAPDH R: AGG GGT CTA CAT GGC AAC TG HPRT F: TGA CAC TGG CAA AAC AAT GCA HPRT R: GGT CCT TTT CAC CAG CAA GCT	FDXR (HS01031617_m1)	DDB2 (Hs00172068_m1), FDXR (HS01031617_m1)	RNA amount used for cDNA synthesis	0.2 µg; 1.65 µg per array
TaqMan® assay: 1×/50°C/2min, 1×/95°C/20s, 45×/95°C/3s, 60°C/30s SYBR Green assay: 1×/95°C/10min, 40×/95°C/15s, 59°C/30s, 72°C/30s, 1×/72°C/1min	1×/95°C/2min, 40×/95°C/10s, 60°C/1min	1×/50°C/2min, 1×/95°C/10min, 40×/95°C/1min, 60°C/1min	cDNA amount used for cRNA synthesis	N.D.
Rotor-Gene Q (Qiagen)	Rotor Gene Q (Qiagen)	QuantStudio™ 12K OA Real-Time PCR System (Thermo Fisher Scientific)	Number of interrogated genes	> 41,000 transcripts
fixed	fixed	0.05	Software	Agilent Feature Extraction Software (v.9.5.1)
TaqMan assay: ITFG1; SYBR Green assay: GAPDH and HPRT geometric mean	HPRT1	Human 18S rRNA (Hs99999901_g1, Thermo Fisher Scientific)	set normalization algorithm	Processed signal value were log2-transformed, normalization via GAPDH
ΔΔ-Ct approach, relative fold change in relation to the 0 Gy sample of the calibration curve	Δ-Ct approach	Δ-Ct approach	Quantification method	Dose estimations based on in-house calibration curves
SYBR Green assay: melting curve inspection			Quality control	Agilent QC report
No	Yes	Yes	Standard curve	not available
No	Yes	Yes	Slope	0,96 - 1,00
No	Yes	Yes	r-sqr	0.99
(-)RT and NTC	HPRT1, (-)RT and NTC	Yes	18s rRNA Cq	not available

TABLE 3
The Table Depicts Team Contributions (from Left to Right) Regarding Employed Genes, Reported Dose Estimates per Reference Sample 1–3, Differences among Reported and Reference Dose-Values as well as the Summed Absolute Difference over all Reference Samples (SAD), a Correct (Yes) or Incorrect (No) Order of Dose Estimates (from Lowest to Highest) Corresponding to Three Dose Categories [Unexposed, Low (1.2 Gy) and Highly Exposed (3.5 Gy)], the Use of *FDXR* Gene Expression Changes for dose estimation, as well as the Report Time

			REPORTED dose estimates		
			Dose estimates (Gy)		
Teams	genes examined	specific features	1 (0 Gy)	2 (1.2 Gy)	3 (3.5 Gy)
4	GADD45A	Calibration samples BIR	**0.0**	5.0	8.4
	FDXR		**0.0**	3.5	5.3
	CDKN1A		0.6	5.1	6.5
	MDM2		1.2	7.6	11.3
	geometric mean		**0.0**	5.1	7.6
	GADD45A	Calibration samples Team 4 A	**0.0**	4.2	9.8
	FDXR		**0.0**	5.1	7.2
	CDKN1A		**0.0**	4.7	7.8
	MDM2		**0.0**	6.0	12.3
	geometric mean		**0.0**	5.0	9.1
	GADD45A	Calibration samples Team 4 B	**0.0**	2.2	5.0
	FDXR		**0.0**	5.1	8.0
	CDKN1A		**0.0**	0.6	**3.4**
	MDM2		**0.0**	3.0	5.8
	geometric mean		**0.0**	2.1	5.3
6	FDXR	Calibration samples BIR	low	medium	high
	FDXR		**0.0**	0.4	4.7
7	**FDXR**	Calibration samples BIR	**0.0**	**0.8**	**3.6**
	DDB2		**0.0**	0.3	0.9
5	FDXR	Calibration samples BIR	low	medium	high
	DDB2		low	medium	high
	FDXR		**0.0**	1.9	>4
	DDB2		**0.0**	0.5	>1
	CDKN1A		**0.0**	**1.3**	1.9
	mean of FDXR and DDB2		**0.0**	1.2	>4
	*mean (**FDXR**, DDB2, CDKN1A)*		**0.0**	**1.3**	**3.0**
2	*8 gene signatures (BAX, BBC3, CDKN1A, DDB2, **FDXR**, GADD45A, GDF15, TNFSF4)*	Calibraton samples BIR and ICHTJ	lowest **0.0**	middle **1.3**	highest **2.8**
1	geometric mean: GDF15, **FDXR**	Calibration RNA aliquots from BIR	**0.0**	**0.9**	1.3
8	FDXR	Own calibration sample	**0.0**	2.0	**4.2**
	*4 gene signatures (**FDXR**, PHLDA3, THC2705989, TNFSF4)*		**0.0**	**1.5**	**4.3**
3	CDKN1A	Calibration samples BIR	**0.2**	2.1	**4.1**
	DDB2		**0.1**	0.6	**2.5**
	FDXR		**0.0**	**0.8**	5.4
	*geom mean (**FDXR,** DDB2, CDKN1A)*		**0.1**	**1.0**	**3.8**
		correct dose estimates	16/16∼100%	8/16∼50%	8/16∼50%
	correct dose estimates related to FDXR		12/16 ∼75%	7/8∼88%	6/8 ∼75%

Notes. The use of different calibration curves and genes generates several dose estimates per team. Reported dose estimates using combined genes are shown in italic. Correct dose estimates considering the accepted uncertainty dose interval for triage dosimetry are given in bold. The number of correct dose estimates and correct dose estimates related to *FDXR* are presented per reference sample and are summed over all reference samples in the lower part of the table.

samples), radiation exposure (X-ray source, Yxlon, Hamburg, Germany), distribution of calibration samples (to all teams except the team performing DNA microarrays) and blinded, coded samples to participating laboratories followed procedures as described in detail in the inter-assay comparison manuscript, of our coordinated article published in this special issue. Comparison between teams was done descriptively using three levels of granularity: (1) precise dose estimates, (2) dose estimates falling within the ±0.5 Gy uncertainty interval for reference doses <2.5 Gy and ±1.0 Gy for reference doses >3 Gy, as introduced for triage biodosimetry (*25*), and (3) allocation of reported dose estimates to reference doses representative for clinically relevant groups.

Sample Preparation and Gene Expression Assays Using qRT-PCR or Microarrays

The Bundeswehr Institute of Radiobiology (BIR) team incubated the irradiated blood samples for 12 h at 37°C, 5% CO_2 (Heraeus BBD 6220) using whole blood, and an equal volume of antibiotic free Roswell Park Memorial Institute (RPMI) 1640 medium containing 10% heat-inactivated fetal calf serum. After washing the blood

TABLE 3
Extended.

REPORTED dose estimates				Correct categorical allocation (unexposed-low, medium, high)	Use of FDXR	Report time hh:mm
Difference (Gy)						
	2	3	SAD (Gy)			
0.0	3.8	4.9	8.7	yes		23:25
0.0	2.3	1.8	4.1	yes	yes	
0.6	3.9	3.0	7.5	yes		
1.2	6.4	7.8	15.5	yes		
0.0	3.9	4.1	8.0	yes		
0.0	3.0	6.3	9.4	yes		
0.0	3.9	3.7	7.6	yes	yes	
0.0	3.5	4.3	7.8	yes		
0.0	4.8	8.8	13.7	yes		
0.0	3.8	5.6	9.3	yes		
0.0	1.0	1.5	2.5	yes		
0.0	3.9	4.5	8.4	yes	yes	
0.0	-0.6	-0.1	0.7	yes		
0.0	1.8	2.3	4.1	yes		
0.0	0.9	1.8	2.7	yes		
				yes	yes	04:43
0.0	-0.8	1.2	2.0	yes	yes	28:51
0.0	-0.4	0.1	0.5	yes	yes	08:36
0.0	-0.9	-2.6	3.5	yes		
				yes	yes	76:52
				yes		122:05
0.0	0.7		nd	yes	yes	264:15
0.0	-0.7		nd	yes		
0.0	0.1	-1.6	1.7	yes		
0.0	0.0		nd	yes	yes	
0.0	0.1	-0.5	*0.6*	yes	yes	
				yes	yes	25:20
0.0	0.1	-0.7	*0.8*	yes	yes	168:54
0.0	-0.3	-2.2	2.5	yes	yes	810:54
0.0	0.8	0.7	1.5	yes	yes	243:30
0.0	0.3	0.8	*1.1*	yes	yes	
0.2	0.9	0.6	1.6	yes		307:01
0.1	-0.6	-1.0	1.6	yes		
0.0	-0.4	1.9	2.4	yes	yes	
0.1	-0.2	0.3	*0.6*	yes	yes	
	25/32 ~ 78.1%					

mixture with EL buffer, cells were lysed in β-mercaptoethanol-RLT buffer (QIAamp RNA Blood Mini Kit, Qiagen) according to the manufacturer's instructions and stored at –20°C overnight. Frozen samples were shipped by overnight courier service on wet ice under defined conditions according to United Nations Regulation 650.

The teams ran assays according to locally established protocols. Quantitative RT-PCR was run by seven teams using different (TaqMan, SYBR Green) chemistries and different sets of genes (Table 1). One team used a DNA microarray platform and either a combination of four genes or only one gene (*FDXR*) for dose estimation. Table 2 provides details for each team regarding RNA isolation, cDNA synthesis and PCR parameters, and details for performing microarrays following the MIQE criteria for publishing gene expression studies (*26, 27*).

After sample receipt, each team isolated total RNA and converted RNA to cDNA according to their protocols as shown in Table 2. Quantitative RT-PCR teams employed different kits for cDNA synthesis, different genes for normalization purposes (e.g., *HPRT* or *18S rRNA*), different radiation-responsive genes either alone or combined (e.g., *FDXR*, *DDB2*, *BAX, CDKN1A, GADD45A*) and different amplification protocols and instruments (Table 2). For analyses, either normalized threshold cycles (Ct-values), relative threshold cycles (Cp-values) or gene expression fold-changes relative to the unexposed control of the calibration curve were employed. Ct-values and Cp-values represent different algorithms to determine a quantitative threshold cycle (Cq-value) along the exponential part of the amplification plot. For convenience, we use only the term Cq-value in this manuscript. Cq-values represent a surrogate for gene

expression changes. They reflect inverse $\log_2$-transformed RNA copy number changes so that, e.g., increased Cq-values (e.g., increase of Cq-values from 16 to 17) represent decreased RNA copy numbers and each additional Cq-value refers to a halving of RNA copy numbers. Seven teams used dose estimates based on 1–4 radiation-responsive genes. Five teams used a combination of 2-8 genes for dose estimation.

Some teams generated calibration samples in addition to the calibration samples sent by BIR. For instance, Team 4 (Table 3) obtained additional blood samples at two time points from a healthy 61-year-old male donor and generated two additional calibration sample sets, resulting in three reported dose estimates based on different calibration curves. These calibration samples were irradiated using a ^{137}Cs γ-radiation source with a dose rate of 0.356 Gy/min. Team 2 combined their own (X-ray irradiation, dose rate: 1.14 Gy/min) and BIR calibration samples into one calibration curve and, thus, one dose estimate was reported per blinded, coded sample (Table 3). Finally, different software tools such as Statistica 9.0 software (StatSoft), GraphPad Prism, version 6.04 (GraphPad Software, La Jolla, CA, USA), R 3.6.2, or Sigma Plot 14.4 (Jandel Scientific, Erkrath, Germany) were employed to fit the calibration curves and to perform dose estimation.

Gene expression analysis using DNA microarrays was performed on the Agilent platform as described previously (*22*). 200 ng total RNA was transcribed into cDNA with an oligo-dT primer, followed by transcription to cRNA labeled with cyanine 3-CTP (Quick-Amp Labeling Kit, One-color, Agilent). cRNA purification was performed with the RNeasy Mini Kit (Qiagen) and dye incorporation and cRNA yields were measured with the NanoDrop-1000 spectrophotometer (Thermofisher). Labeled cRNA samples were applied on the DNA microarray slides (44k whole human genome, G4112F, Agilent). For hybridization, DNA microarrays were placed into a hybridization oven (Agilent) at 65°C for 17 h. After hybridization, DNA microarrays were washed, and slides were immediately scanned with the Microarray Scanner (G2505 B, Agilent) as recommended by Agilent. The preprocessing procedure and subsequent statistical analysis were applied separately using Agilent Feature Extraction Software Version 9.5.1. The processed signals (Agilent gProcessedSignals including background subtraction) were subsequently $\log_2$-transformed and normalized via GAPDH. Dose estimation was performed using a 4-gene signature as well as one gene (*FDXR*) employing internal in-house calibration curves (*11, 22, 23*).

Further details on each method are provided in the Supplementary Materials[1] (https://doi.org/10.1667/RADE-22-00206.1.S1).

Statistical Methods

Differences (for examining over- or underestimation) as well as absolute differences (AD, allowing for quantitative comparisons per reference sample) of estimated doses to their corresponding reference doses were calculated considering the uncertainty intervals introduced for triage dosimetry as outlined above. Reported dose estimates lying within corresponding reference dose intervals are named ''correctly'' reported dose estimates within this manuscript. For a more aggregated comparison of the teams' contributions, the differences between estimated and reference doses over the three reference exposures were summed and are called *summed absolute difference* (SAD). In addition, allocation of reported dose estimates to reference dose groups corresponding to clinically relevant groups was examined. These groups comprised unexposed (no clinical resources required), low dose exposed (1.2 Gy group, no hospitalization required) and high dose exposed individuals (3.5 Gy group, immediate and intensive care required). Group comparisons were performed using either the t-test or Mann-Whitney Rank sum tests, where applicable. All calculations were performed using either SAS (release 9.4, Cary NC) or Excel (Microsoft Corporation). Graphs were created using Sigma Plot 14.5 (Jandel Scientific, Erkrath, Germany). Linear or linear-quadratic curve fits were performed where applicable (Sigma Plot 14.5). Supplemental File 1 includes more statistical details for each team where required.

[1] Editor's note. The online version of this article (DOI: https://doi.org/10.1667/RADE-22-00206.1) contains supplementary information that is available to all authorized users.

RESULTS

Participating Institutions, Contributions and Reported Dose Estimates

Table 1 provides an overview on the platforms, genes and calibration samples used by the eight teams. Further methodological details are summarized in Table 2. Team numbers in Table 1 are the same throughout all figures and tables to better follow results and workflow characteristics. Eight teams (Table 1) provided a total of 105 dose estimates (Table 3). For instance, Team 4 provided dose estimates based on four genes (*GADD45A*, *FDXR*, *CDKN1A*, *MDM2*) and their geometric mean, using three different calibration curves. This generates five dose estimates per blinded, coded sample and calibration curve and a total of 45 (5x3x3) reported dose estimates (Table 3).

Team 8 using a DNA microarray platform estimated the dose based on a previously developed algorithm using a gene set consisting of 4 genes (*TNFSF4*, *FDXR*, *PHLDA3*, *THC2705989*) (expressed sequence tag with a yet unknown function) and *FDXR* only (*22, 23*). No further calibration samples were required. Instead, internal calibration curves of the four signature genes were used. The derived expression values of the four signature genes in sample 1 (0 Gy) of the blinded, coded RNA samples were similar to or slightly below the values of the non-irradiated controls of the internal in-house calibration curves. The two contributions (4-gene signature and *FDXR* alone) resulted in two dose estimates per blinded, coded sample and a total of 6 dose estimates (Table 3).

The earliest report times of categorical and precise dose estimates were around 5 h and 9 h, respectively (Table 3). Further dose estimates were reported within 3 days and five teams provided dose estimates later. The median report time was about 10 days (244 h) and included groups that did not process these samples with priority.

Methodological Accuracy of qRT-PCR

The accuracy of qRT-PCR gene expression measurements was examined using the technical replicates run in duplicate/triplicates and/or performed by two experts. In the case of microarrays, no replicate measurements of calibration samples were performed. The coefficient of variation (CV, standard deviation relative to the mean RNA copy number) for 84.6% and 58.9% of all 436 measurements did not exceed 10% and 5%, respectively (see horizontal dotted lines in Fig. 1). Lower CVs ($<5\%$) were observed for most measurements produced by two of the teams (left side, Fig. 1). Three other teams (middle, Fig. 1)

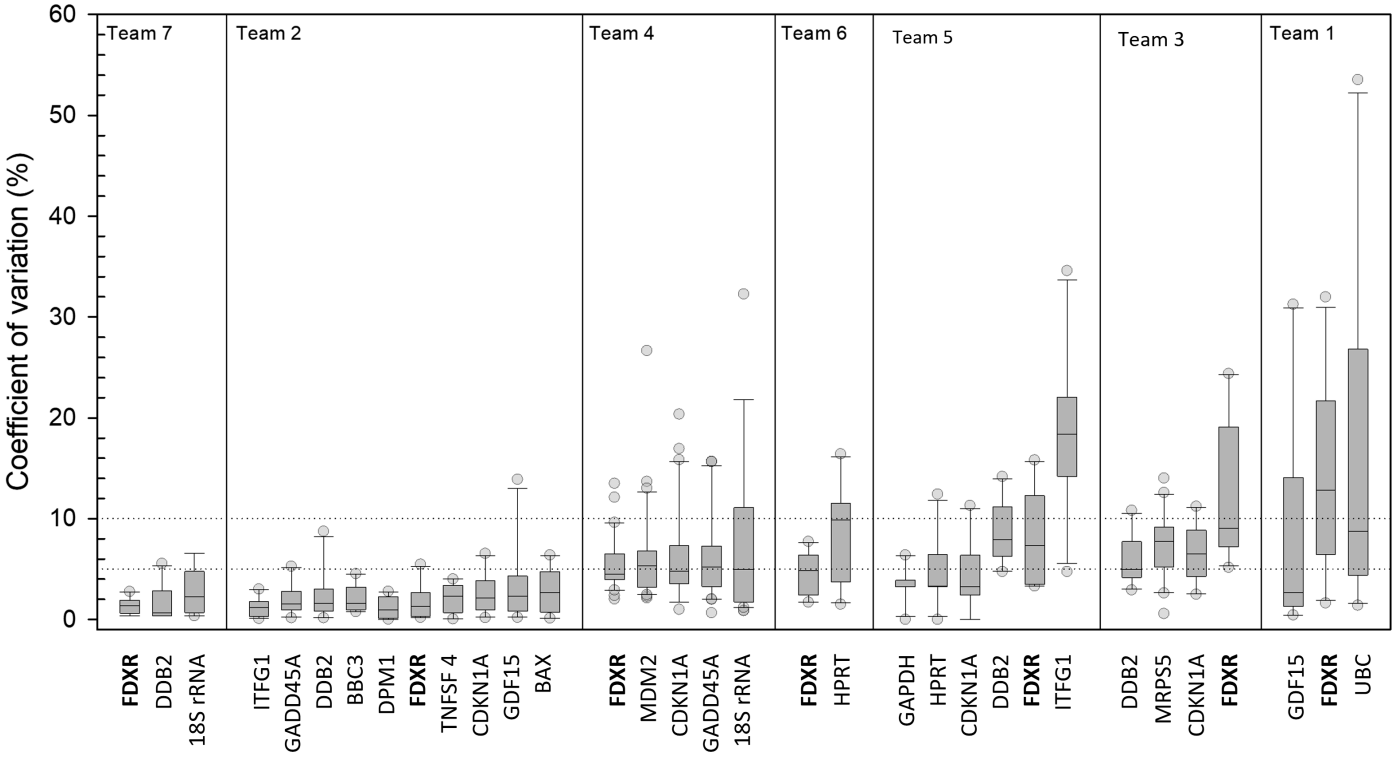

FIG. 1. The coefficient of variation (CV) was calculated based on all available technical replicates and genes. The distribution of CVs per gene is reflected by a box plot showing the 10th (lower whisker), 25th (lower end of the box), 50th (median, straight line), 75th (upper end of the box) and 90th (upper whisker) percentiles. Genes are ordered with increasing raw Cq-values. Teams are numbered as outlined in Table 1.

produced CVs for most genes ranging between 5–10%, while CVs exceeding 10% were calculated for one team (right side, Fig. 1). *FDXR* was the only gene used either alone or in combination by all teams (Fig. 1, Table 3).

Calibration Curves and Reported vs. Reference Dose Estimates

Teams plotted gene expression values versus dose in different ways. For instance, two teams plotted normalized Cq-values of a combination of genes and aggregated values either by applying a geometrical mean or building a sum (Fig. 2A and B). In most cases, teams plotted normalized Cq-values of single genes (e.g., *FDXR*) vs. dose either using linear scales (Fig. 2C and D) or log-scales (Fig. 2E). Plotting Cq-values and dose on log-scales facilitated a linear regression model covering most of the variance ($r^2 = 0.99$) as opposed to other approaches where a linear regression model diverged from the calibration values (e.g., $r^2 = 0.59$, Fig. 2C). For normalized Cq-values increased copy numbers of radiation-induced genes resulted in a negative slope of the calibration curves. When using unexposed calibration samples as the reference (value = 1), differential gene expression increased with increasing radiation dose, resulting in a positive slope of the calibration curve (Fig. 2F and G). Unexposed dose estimates (referred to as ''1'' in Fig. 2) in some plots appear above the calibration curve (e.g., Fig. 2A and E). They are referring to negative dose estimates. To avoid extension of the x-axis into the negative dose range, these samples are plotted above the calibration curve and are referring to the 0 Gy (linear scale) or 0–0.01 Gy dose range (log scale). A saturation in gene expression values was observed between 3–4 Gy for most calibration curves or even at 2 Gy (Fig. 2A).

The unexposed control sample (sample 1) was correctly estimated to be in the range between 0 and 0.5 Gy by all teams except Team 4, where 2 out of 12 dose estimates were not in this range (Fig. 3, Table 3). Differences to the reference dose were zero in all except two dose estimates which belonged to Team 4 (Fig. 3A and B). Reported dose estimates of 1.2 Gy (Fig. 3C and D) and 3.5 Gy (Fig. 3E and F) irradiated samples were systematically overestimated by Team 4, while other teams provided dose estimates close to the reference dose as well as over- and underestimations with a trend to an underestimation observed at 3.5 Gy exposures in three teams (Fig. 3 F).

Altogether, 50% of the reported dose estimates were within the accepted uncertainty interval for triage dosimetry regarding the 1.2 Gy and 3.5 Gy irradiated blinded, coded samples (see bold dose estimates and calculations in lower part of Table 3). The dose estimates from all teams correctly identified the ordering with regard to the dose effect relationship of the blinded, coded samples (lowest, middle,

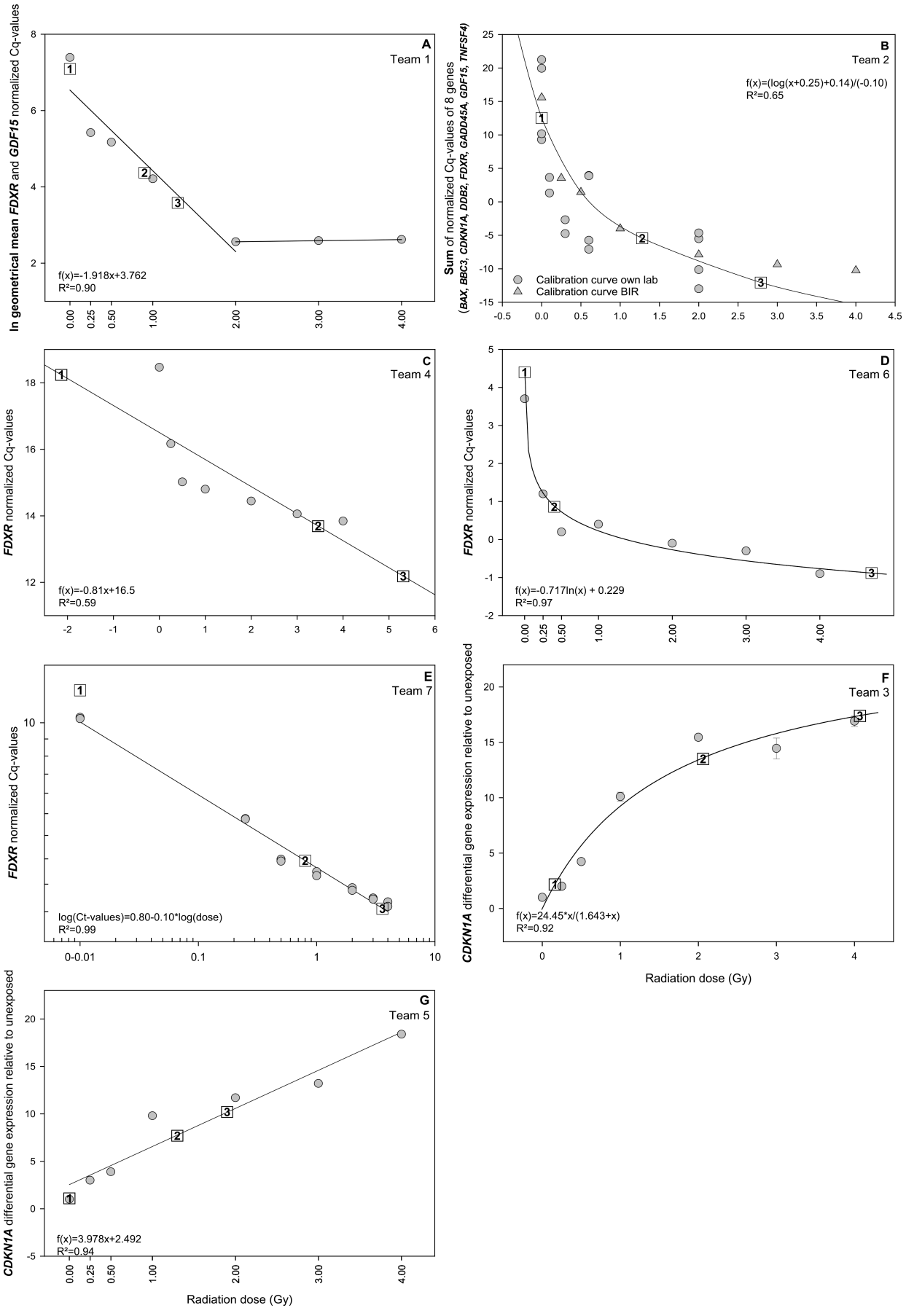

highest exposures), using all reported and semiquantitative dose estimates (Table 3).

Reported dose estimates using contributions from all teams revealed overlapping dose estimates among unexposed, low, and highly exposed groups, which hindered their discrimination (Fig. 4 A). Overlapping reported dose estimates between exposure groups were reduced after exclusion of Team 4's contributions (Fig. 4 B) and using reevaluated dose estimates generated from newly synthesized cDNA of BIR calibration samples (Fig. 4 C). This resulted in reported dose estimates that identified unexposed and highly exposed samples with 100% certainty, meaning that if the dose estimate predicted 0 Gy or 3.5 Gy, in all cases the corresponding samples belonged to the unexposed or highly exposed clinical group, respectively (Fig. 4 B and C, arrows). Reported dose estimates below 3.5 Gy could not discriminate between the low (1.2 Gy) and the highly (3.5 Gy) exposed group in most cases (Fig. 4 B and C).

Team 4 Contributions

Team 4 experienced a systematic shift of dose estimates towards higher values (Table 3, Fig. 5A, B), so these results were examined more closely. Dose estimates were derived using either BIR calibration samples or two additional sets of calibration samples generated by Team 4, which differed from the BIR calibration samples regarding the radiation exposure, as well as donors age and sex (Fig. 5C). Reevaluation of *FDXR*-based dose estimates performed after the exercise by the same team were 0 Gy, 2.2 Gy and 2.8 Gy (using the raw Cq-for the reported BIR calibration samples), 0 Gy, 2.0 Gy and 3.0 Gy (using new cDNA of BIR calibration samples), and 0 Gy, 2.3 Gy and 3.6 Gy (using normalized Cq-values from re-run reported BIR calibration samples) corresponding to the 0, 1.2 and 3.5 Gy irradiated blinded, coded samples (Fig. 5).

Reasons for this discrepancy were most likely technical issues, either pipetting error, primer dilution and/or use of defective mastermix for certain samples, which impaired the accuracy of the 18S rRNA Cq-values obtained during the reporting of dose estimates, and, in turn, had a negative impact on reported normalized Cq-values. This was concluded since dose estimates using raw Cq-values from reported dose estimates provided better dose estimates than after normalization (Fig. 5A, B), and that 18S rRNA Cq-values obtained within the exercise for blind samples no. 2 and no. 3 were higher compared to additional runs performed after the exercise. This in turn resulted in lower reported normalized Cq-values, and consequently higher dose estimates as compared to those observed using newly synthesized cDNA, where both blind coded samples no. 2 and no. 3 did intersect the BIR calibration curve (Fig. 5A). Additionally, re-run of qPCR using the same cDNA used for the reported *FDXR*-based dose estimates using BIR calibration samples and Team 4 calibration A samples (insufficient material to re-run calibration B samples), resulted in similar dose estimates to those derived from the newly synthesized cDNA after the exercise for all calibration samples, and also from raw Cq-values from reported data in the case of BIR samples (Fig. 5A). Moreover, 1:2 dilution of 18S rRNA leading to raw Cq-values of 9 seem to represent Cq-values within the linear dynamic range of the method and do not explain the observed discrepancies (Supplementary Materials; https://doi.org/10.1667/RADE-22-00206.1.S1). Also, dose estimates based on the *GADD45A*, *CDKN1A* and *MDM2* genes improved after the exercise using either raw Cq-values for reported or new cDNA (Fig. 5B). A lower magnitude of gene expression, i.e., higher Cq-values, with early saturation at approximately 1–2 Gy was observed for the additionally generated two calibration sample sets of Team 4 resulting in higher dose estimates as compared to those derived from BIR calibration samples, which presented a later saturation at approximately 4 Gy (Fig. 5C). Additionally, fitting the curvi-linear dose-to-Cq-value-association with a linear regression model introduced deviations from the reference doses (Fig. 2C), yet the use of a linear quadratic model to fit the reported normalized Cq-values (Fig. 5A) would have made the dose estimation of blind sample no. 3 impossible. Finally, the Cq-value difference calculated within the 0–4 Gy dose band of irradiated calibration samples converted into fold changes in gene expression of 3–4 fold for *GADD45A* and *MDM2*, 3–14 fold for *CDKN1A* and 13–23 fold for *FDXR*, making *FDXR* the most promising candidate gene, based on increased robustness in the detection of high fold changes (Fig. 5C). Also, BIR calibration samples provided significantly higher fold changes for all genes compared with the two calibration sets generated by Team 4 ($P = 0.01$).

←

FIG. 2. Calibration curves were generated before the exercise by seven teams and those shown herein represent typical examples. Either multiple (panels A and B) or single gene (panels C–G) expression changes are plotted versus the known radiation doses. Gene expression values are often given as raw or normalized Cq-values or as a fold change (panels F and G) using unexposed samples as the reference. The presented formula in panel 1 (Team 1) refers to the gene expression response after 0–2 Gy and excludes higher doses where the response saturates. Further details on fitting of data are presented in Supplementary Materials S1 (https://doi.org/10.1667/RADE- 22-00206.1.S1). Circles represent mean gene expression values from technical replicates. Error bars represent standard deviation of duplicate measurements (and standard error of mean in panel F) and are visible when larger than the symbols. Reported dose estimates are plotted as squares and numbers 1, 2 and 3 refer to unexposed, 1.2 Gy and 3.5 Gy irradiated blinded, coded samples, respectively. Unexposed (no. 1) dose estimates are sometimes not plotted on but above the calibration curve, referring to negative dose estimates. To avoid extension of the x-scale into the negative dose range, these samples are plotted above the calibration curve and are referring to the 0 Gy (linear scale) or 0–0.01 Gy dose range (log scale). Teams are numbered as outlined in Table 1.

Using Single Genes, FDXR, and Combined Gene Signatures for Dose Estimation

FDXR was employed by all teams and 17 out of 35 dose assessment approaches employed *FDXR* either alone or combined with other genes (Table 3). Altogether 78.1% of correctly reported dose estimates made use of *FDXR* gene expression measurements (see calculations in the lower part of Table 3). Also, reported dose estimates (excluding Team 4) based on a gene combination provided more precise dose estimates (median SAD of 0.8 Gy, ±0.8 Gy) than those employing a single gene, e.g., *CDKN1A* or *DDB2* (median SAD of 1.7 Gy, ±0.8 Gy) or *FDXR* only (median SAD of 1.8 Gy, ±0.8 Gy, Fig. 6). Interestingly, when reported separately, difference of *FDXR* based reported versus reference doses (marked as stars in Fig. 3F) was consistently above 0 for the 3.5 Gy reference sample. The lowest *FDXR* based SAD of 0.5 Gy was accomplished by Team 7 with an accuracy comparable to teams combining several genes for dose estimation (Table 3, Fig. 6).

Testing for Improvements in Dose Estimations Using Remaining RNA and cDNA Samples when Employing the Same Workflow (After-Exercise Experiments)

Six teams entrusted remaining isolated RNA (n = 5) or synthesized cDNA (n = 3) of calibration curves and blinded, coded samples for further study following the workflow of Team 7 (Fig. 7) to elucidate the impact of a similar workflow on the accuracy of dose estimates. Employing the same workflow (from Team 7) to the 1.2 Gy and 3.5 Gy reference samples decreased the absolute differences (ADs) relative to the employment of different workflows in three of the entrusted RNA/cDNA samples, while increasing the ADs in three other RNA/cDNA samples (Fig. 8, underlying details are shown in Supplementary Fig. S1; https://doi.org/10.1667/RADE- 22-00206.1.S2). Improved ADs were more pronounced at 3.5 Gy. Here, ADs employing the same workflow were roughly halved over RNA/cDNA samples processed using different workflows. In contrast, the 1.2 Gy and 3.5 Gy blinded, coded RNA samples originating from Teams 3 and 6 did not gain, i.e., SADs became larger, from the employment of the same workflow (Fig. 8).

DISCUSSION

Large-scale radiological or nuclear events require preparedness measures (*28*). Since its foundation in 2012 (*29*) RENEB performs inter-laboratory comparison (ILC) exercises for validating assay performance as well as laboratories for individual biodosimetry purposes (*1–11*).

For gene expression assays in the current exercise, reported dose estimates were provided within hours after sample delivery, demonstrating this methodology's early and high-throughput capability as shown before in a NATO ILC (*14*). Also, if performed accurately, this methodology bears a high accuracy and even CVs below 5 % can be reproduced by some teams, which is in agreement with cited work (*2*).

In the current ILC some teams employed an unexposed reference for dose estimation and other teams used normalized gene expression changes, exemplifying that dose estimates can be generated even without a pre-exposure control (Fig. 2). Employing this assay for dose estimation in the absence of a matched pre-exposure control is another desirable feature of gene expression measurements for dose estimation and is in agreement with previous findings (*19*).

Of note, *FDXR* was used by all teams, and 78% of correctly reported dose estimates [considering the uncertainty dose interval for triage dosimetry) were based on *FDXR* measured either solely or in combination with other genes (Table 3). *FDXR* has been already recognized as a promising gene for dose estimation (for review, see the literature (*2, 17, 24, 30, 31*)]. However, using one gene only for dose estimation (including *FDXR*) seemed to reduce robustness compared with the combination of certain gene sets and the median summed absolute difference (SAD) calculated over all three blinded, coded reference samples approximately doubled relative to teams employing a combination of genes (Fig. 6). However, the variance was high, the number of measurements was low, and differences between groups were not significant. Future experiments are required for final judgment on the issue of using one versus several genes for dose estimations (32).

Interestingly, Team 7, using *FDXR* as a single gene for dose estimation, performed comparably (SAD = 0.5 Gy) to teams using a gene set (SAD = 0.6–1.1 Gy; Table 3). This motivated us to examine whether a similar preparation and analysis starting from entrusted remaining RNA and cDNA samples from other teams would result in improved reported dose estimates. Six teams sent RNA and cDNA to Team 7, and all samples were processed and analyzed similarly. Somewhat unexpectedly, only half of the measurements improved and the others did not (Fig. 8). Since all cDNA samples (except for Teams 1 and 2) were prepared and analyzed similarly in this additional experiment, RNA isolation (and cDNA synthesis for two teams) differently performed by the teams might explain the discrepancies found. Also, some teams entrusted low amounts of RNA or cDNA left after the exercise for further analysis, which challenged the workflow. It is possible that further RNA degradation occurred during return shipping, which may have impacted the data. However, improved dose estimates certainly were obtained by application of a common regression model for fitting the calibration data. Comparison of calibration curves between teams and differences in explained variance of chosen regression models (e.g., 59% vs. 99%; Fig. 2) argue for that. In this context, a log-transformation increased the explained variance over, e.g., linear models (Fig. 2). This was accomplished by reducing the resolution in the lower dose range. Consequently, doses ranging between 0–0.01 Gy cannot be discriminated.

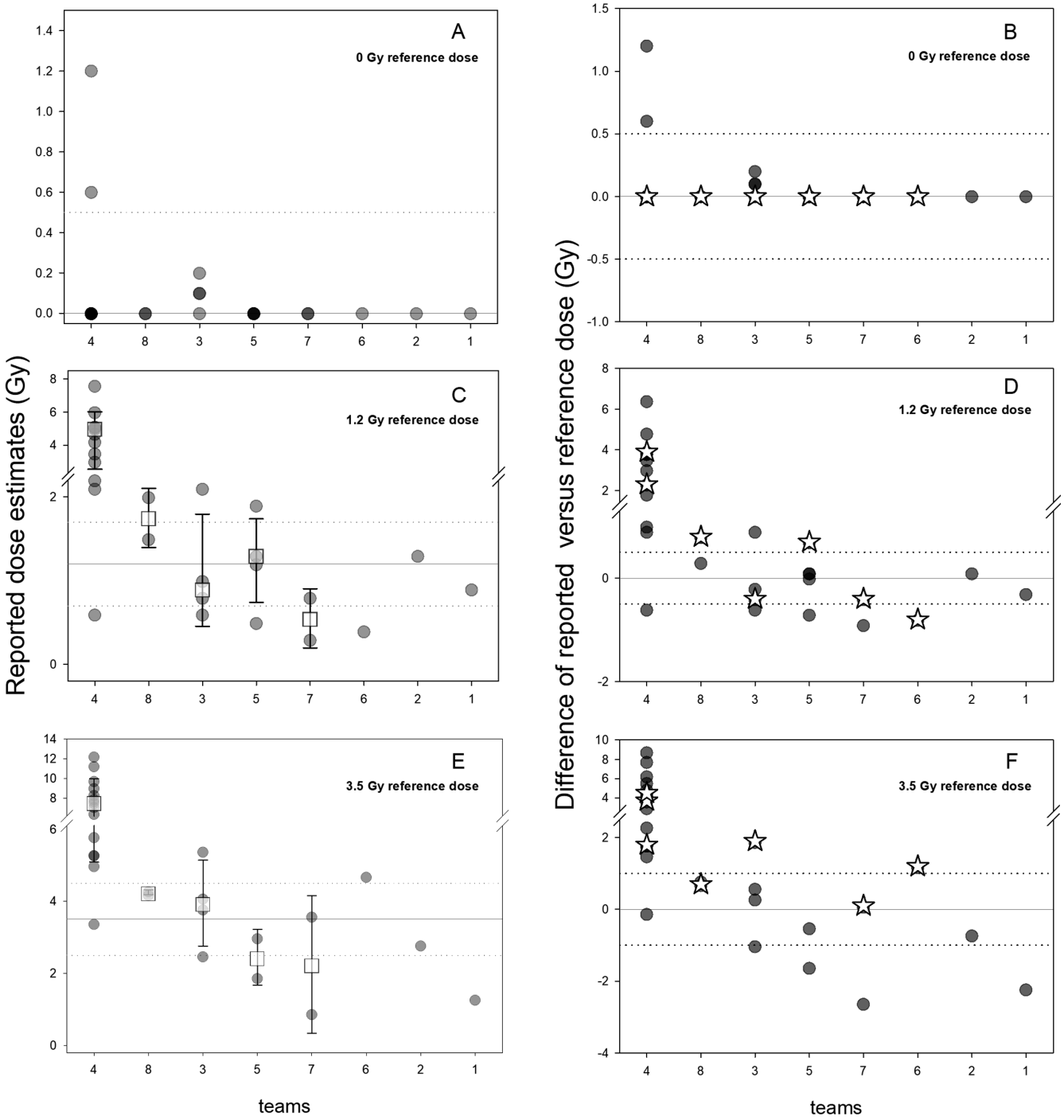

FIG. 3. Reported dose estimates are provided per team (teams are numbered as outlined in Table 1) on the left panels and corresponding differences of reported versus reference doses are shown in the right panels. The panels A, C, and E reflect reported dose estimates corresponding to the unexposed, 1.2 Gy and 3.5 Gy irradiated samples, respectively. Panels B, D, and F reflect corresponding differences of reported versus reference doses. Dotted lines refer to the ±0.5 Gy (reference doses below 2.5 Gy) and ±1 Gy (reference doses >3 Gy) uncertainty interval for dose estimation of triage dosimetry. Solid lines reflect values of the reference dose. Circles represent reported dose estimates and squares reflect mean values with error bars showing the standard deviation. Results are provided in descending order of mean reported dose estimates. Stars correspond to dose estimates based on gene expression changes using *FDXR*.

Furthermore, if teams reported no exposure or an exposure >3.5 Gy, it was always correctly allocated to the unexposed or the highly exposed group, which represents a strong contribution to the medical management in radiological or nuclear scenarios (Fig. 4). However, dose estimates below 3.5 Gy in most cases could not discriminate the 1.2 Gy from the 3.5 Gy reference samples, which points to limitations of this approach.

An advantage of this inter-laboratory comparison is the easy detection of technical problems in the use of qRT-

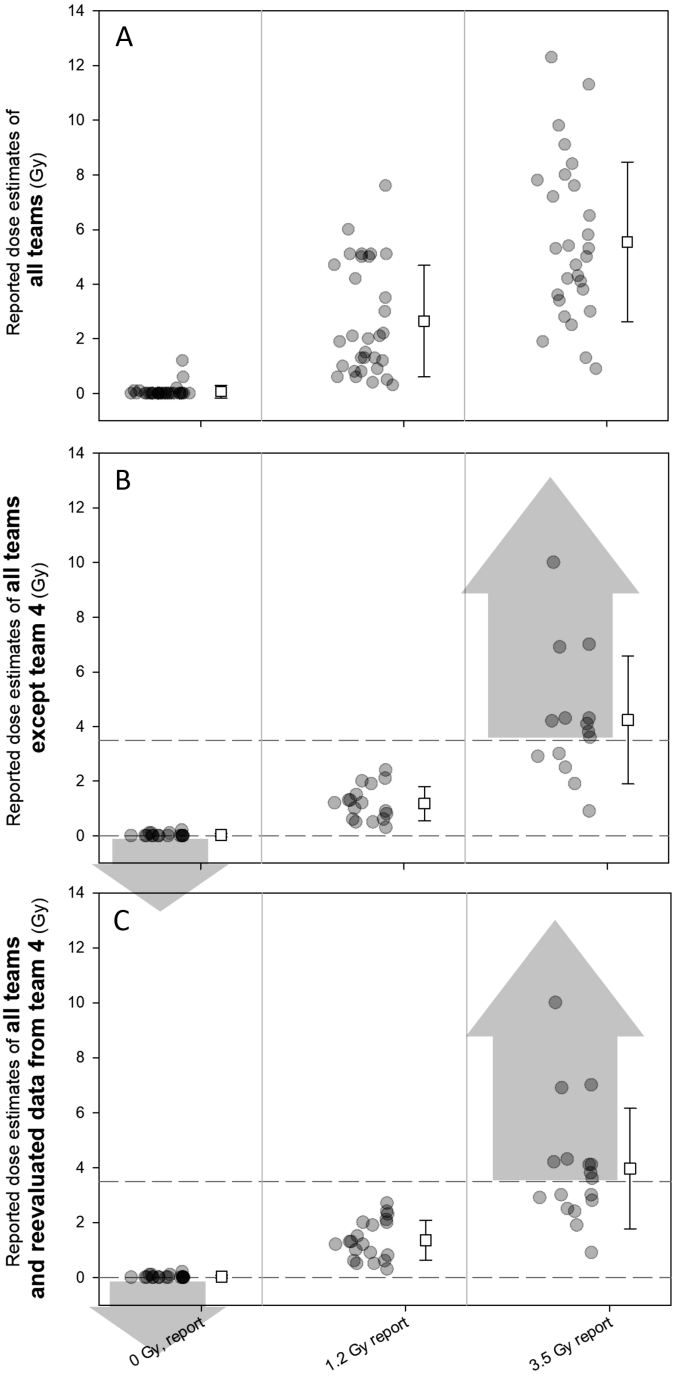

FIG. 4. Reported doses estimates of all teams and corresponding dose categories (x-scale) are shown in panel A. Panel B reveals the same data, excluding dose estimates from Team 4. Panel C comprises reported dose estimates of all teams as well as reevaluated dose estimates from Team 4 generated on normalized Cq-values of newly synthesized cDNA from BIR calibration samples as provided in Fig. 5B. Circles represent reported dose estimates and squares reflect mean values with error bars showing the standard deviation. Arrows in panels B and C are related to unexposed and highly exposed groups. They reflect reported dose estimates (0 Gy and $\geq$3.5 Gy, represented by horizontal dashed lines), where dose groups are identified correctly and without misclassification.

PCR, including data analysis, leading to differences in dose estimates. For instance, Team 4 observed systematic overestimation in reported dose estimates (Fig. 3). However, reevaluation after the exercise provided dose estimates similar to the reference samples (Figs. 4C and 5). This discrepancy was probably attributable to methodological issues (pipetting error, malfunctioning master mix), using a regression model that insufficiently fit calibration values, and the use of several genes (*GADD45A, MDM2*) responding with low changes in copy numbers after irradiation relative to *FDXR* (Figs. 2 and 5). Furthermore, the two sets of calibration samples generated by Team 4 revealed unusual saturation in gene expression after 1–2 Gy radiation exposure, which was absent in the BIR calibration samples. Differences regarding radiation quality (X rays vs. γ rays) and dose rate (1 Gy vs. 0.356 Gy/min) are known to impact gene expression changes and might have contributed here (*33, 34*). Also, Team 4 calibration samples originated from a 61-year-old male, but BIR calibration samples originated from a 30-year-old female. Age and sex dependent changes in gene expression are reported (*35*), but are probably of minor significance in explaining the differences in dose estimates reported here.

Furthermore, both Team 4 and Team 7 employed 18S rRNA as a housekeeping gene, with the difference that while the former team used a dilution factor of 1:2, Team 7, given 18S high abundance, used a dilution factor of 1:1,000 to ensure a Cq-value lying well within the linear dynamic range of their method. Despite the low Cq-values obtained for the 18S rRNA by Team 4, the linearity of the method in this range was also validated (Supplementary Materials S1; https://doi.org/10.1667/RADE- 22-00206.1.S1). It was an experience of this exercise that depending on the platform used, the linear-dynamic range can shift considerably to lower or higher Cq-values. Dilution of 18S rRNA represents an additional burden of that housekeeping gene and if unexperienced can introduce larger standard deviations, but unaltered 18S rRNA copy numbers after irradiation and similar copy numbers observed in different tissues and species outweigh this concern (*36, 37*).

The identified problems and measures taken to improve the precision of dose estimates clearly demonstrate the added value of running ILC exercises by laboratories involved in biological dosimetry and argue in favor of a further standardization of research protocols.

This RENEB ILC gene expression assay exercise bears some limitations. For instance, blinded, coded samples were taken from one healthy donor only. Thus, inter-individual and biological variability (e.g., caused by diseases or demographic factors) were not assessed. Nevertheless, for the overall exercise, this allowed 86 teams worldwide to participate, employing physical as well as cytogenetic and molecular biological based dosimetry assays. In addition, calibration samples (originating from a female, healthy donor) were provided using the same radiation source and were generated before the irradiation of blinded, coded

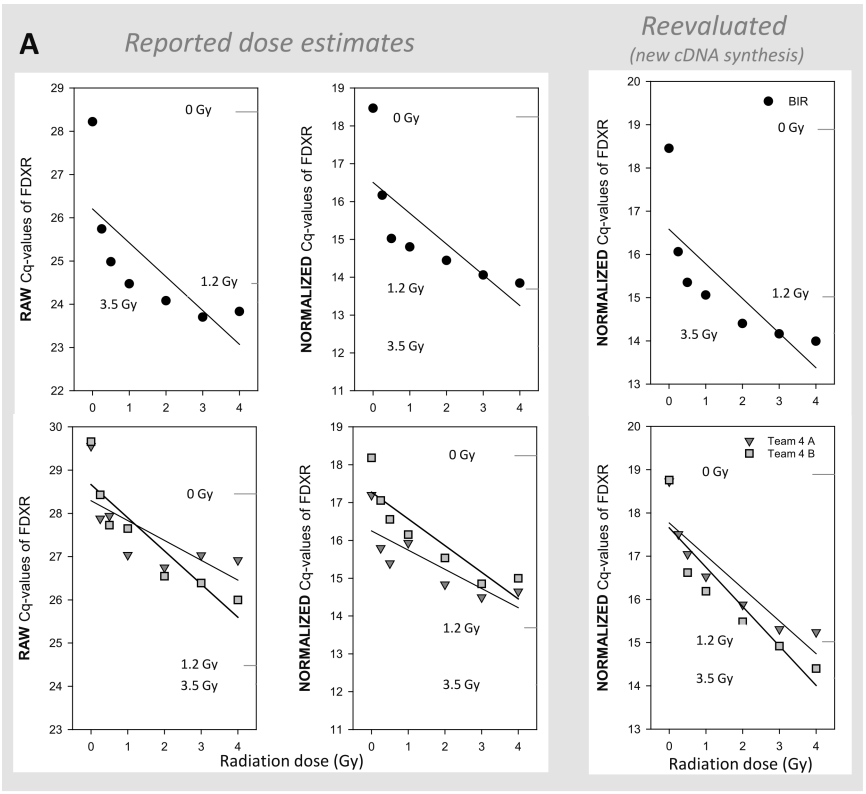

B

Gene	Calibration samples	Blinded coded samples (Gy)	Reported dose estimates (Gy) raw Cq	Reported dose estimates (Gy) normalized	Reevaluated dose estimates (Gy) Remaining cDNA raw Cq	Reevaluated dose estimates (Gy) Remaining cDNA normalized	Reevaluated dose estimates (Gy) New cDNA, normalized
FDXR							
	BIR		0	0	0	0	0
	Team 4 A	**0**	0	0	0	0	0
	Team 4 B		0.3	0			0
	BIR		2.2	3.5	1.5	2.3	2
	Team 4 A	**1.2**	8.3	5.1	4.2	4	3.6
	Team 4 B		5.5	5.1			2.9
	BIR		2.8	5.3	2.7	3.6	3
	Team 4 A	**3.5**	9.3	8	5.3	5.1	4.7
	Team 4 B		6	7.2			3.8
CDKN1A							
	BIR		0	0.6			0
	Team 4 A	**0**	0	0			0
	Team 4 B		0	0			0
	BIR		3.8	5.1			2.3
	Team 4 A	**1.2**	4.6	0.6			0
	Team 4 B		5.4	4.7			0.7
	BIR		3.7	6.5			2.8
	Team 4 A	**3.5**	4.5	3.4			0.8
	Team 4 B		5.3	7.8			1.2
GADD45							
	BIR		0	0			0
	Team 4 A	**0**	1.8	0			0
	Team 4 B		0.1	0			0
	BIR		2.3	5			0.9
	Team 4 A	**1.2**	5.6	2.2			1.8
	Team 4 B		5.4	4.3			0
	BIR		2.9	8.4			2.4
	Team 4 A	**3.5**	6	5			3.1
	Team 4 B		6.1	9.8			1
MDM2							
	BIR		0	1.2			0
	Team 4 A	**0**	2.3	0			0
	Team 4 B		0.6	0			0
	BIR		5	7.6			2.7
	Team 4 A	**1.2**	6.3	3			3.5
	Team 4 B		6.8	6			0
	BIR		5.7	11.3			4.1
	Team 4 A	**3.5**	6.8	5.8			5.1
	Team 4 B		7.7	12.4			1.4

C

Calibration samples	Exposure	Age	Gender	*Maximal gene expression fold-change* *FDXR*	*CDKN1A*	*GADD45A*	*MDM2*
BIR	X-ray, 1 Gy/min	30	female	22.6	13.9	3.5	3.5
Team 4 A	^{137}Cs, 0.36 Gy/min	61	male	7.0	3.0	2.7	4.0
Team 4 B	^{137}Cs, 0.36 Gy/min	61	male	13.0	4.6	2.8	3.0

FIG. 5. Here we show Team 4 data. Panel A reflects *FDXR* gene expression changes plotting raw (left graphs) and normalized Cq-values (middle graphs) of reported dose estimates using either BIR (Bundeswehr Institute of Radiobiology) calibration samples (top panels), or two sets of calibration samples generated by Team 4, termed Team A and Team B (bottom panels), respectively. Panels to the right represent reevaluated data generated on newly synthesized cDNA of RNA extracted from calibration samples as indicated. Dashed horizontal lines refer to Cq-values corresponding to blinded, coded samples no. 1 (0 Gy), no. 2 (1.2 Gy), and no. 3 (3.5 Gy) as indicated in the panels. Panel B shows dose estimates generated both during (left) and after the exercise (right) based on the different calibration curves used by Team 4 for *FDXR*, *GADD45A*, *CDKN1A* and *MDM2* genes. ''Reported dose estimates'' corresponds to dose estimates determined during the exercise, and dose estimates based on raw and normalized Cq-values are shown. ''Reevaluated dose estimates'' include dose estimates generated after the exercise. It comprises raw and normalized Cq-values generated from remaining cDNA as used for the reported dose estimates as well as data generated from newly synthesized cDNA. The table in panel C reflects exposure, age and sex differences between the different sets of calibration samples employed as well as a calculation of fold-differences among the four genes examined, which were generated at the dose which created the maximal fold change from 0–4 Gy irradiated calibration samples employing the 0 Gy Cq-values as the reference.

samples. The unirradiated blind sample would be missing in a real case scenario, but a calibration sample could be arranged or stored beforehand, provided the type of source is known. However, correct categorical classifications of clinical groups, over all teams and all approaches used, support the view that this might be achievable even without calibration samples but employing a laboratory's own reference samples, as already demonstrated by two teams in this exercise. Indeed, this has to be proven in the context of another exercise. In this regard, identifying clinical categories of exposed individuals and predicting the severity of acute health effects based on semiquantitative changes in gene expression of four genes (*FDXR, DDB2, POU2AF1, WNT3*) has been introduced recently (*37*). This approach of predicting the severity of the expected health effects and not the magnitude of the exposures (dose) might provide another avenue complementary to the dose estimation approach.

In summary, this ILC exercise enabled: 1. identification of technical problems and corrections in preparation for future events, 2. confirmed the early and high-throughput capabilities of gene expression, 3. emphasized different biodosimetry approaches using either only *FDXR* or a gene combination, 4. indicated some improvements in dose estimation with *FDXR* when employing a similar methodology, which requires further research for final conclusion and 5. underlined the applicability of gene expression for identification of unexposed and highly exposed samples,

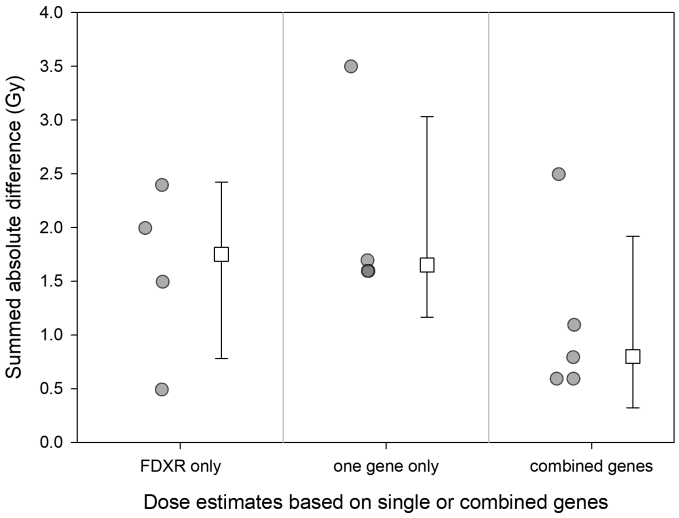

FIG. 6. The summed absolute difference (Gy) was plotted depending on the application of single genes for dose estimation (*FDXR* only, other single genes, left and middle part of the graph) or the use of a combined set of genes (right side). Circles represent reported dose estimates and squares are reflecting median values with error bars showing the standard deviation.

supporting medical management in radiological or nuclear scenarios.

SUPPLEMENTARY MATERIAL

Supplementary Material S1. Details on methods and statistics of contributing laboratories where required.

Supplementary Fig. S1 Four teams provided RNA (left graph) and two teams cDNA (right graph) for further processing and analysis by Team 7. Only *FDXR* gene expression was measured, and only BIR calibration samples and no calibration samples of other origin were examined. Both *FDXR* normalized gene expression (Cq-values) of calibration and blinded, coded samples as well as radiation dose were plotted on logarithmic scales. The 0.01 Gy value refers to the 0–0.01 Gy dose band. Linear regression was used for connecting calibration samples (rsq$\geq$ 0.98). The same symbols refer to the same RNA from one team, but calibration samples are shown as white and blinded, coded samples with dark grey fills. Error bars represent standard deviation of duplicate measurements and are visible when

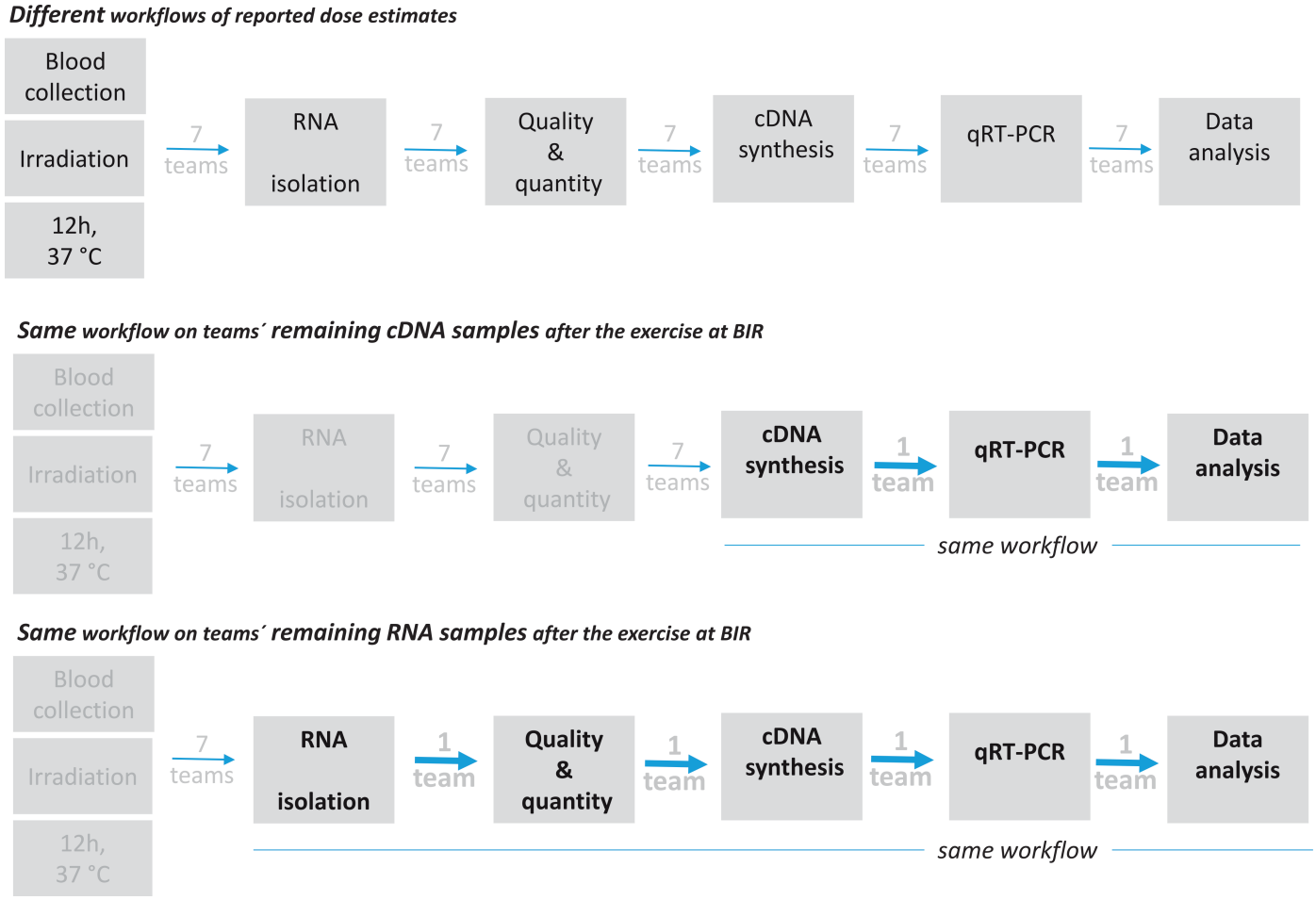

FIG. 7. Overview of samples prepared at BIR (Bundeswehr Institute of Radiobiology), sent to the participants, and processed by the Teams no. 1–7 starting with isolation of RNA after the arrival of lysed peripheral blood aliquots (upper row). The reported dose estimates were generated based on these different workflows of the teams. To further elucidate the origin of differences in reported dose estimates among teams, either cDNA (second row) or isolated RNA (third row) was entrusted by six teams to the team showing reported dose estimates closest to the reference doses. The same workflow and its impact on dose estimates was applied to entrusted cDNA (middle row) and RNA (lower row).

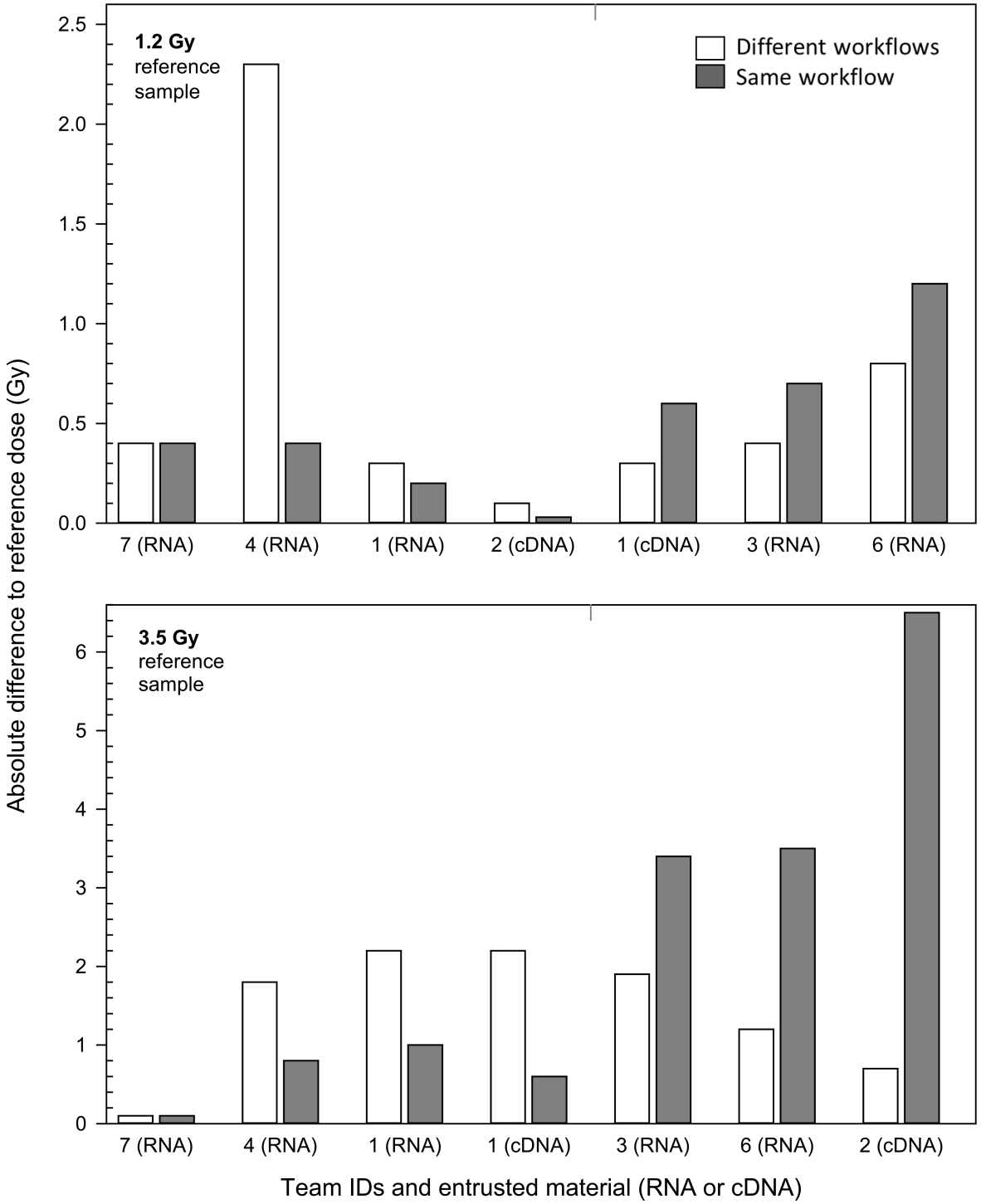

FIG. 8. The absolute difference (Gy) was compared per team employing either the different workflows established at Team 1–7 laboratories (white bars) or applying the same workflow for entrusted RNA or cDNA samples by one team (gray filled bars). *FDXR* gene expression changes after a reference dose of 1.2 Gy (upper panel) and 3.5 Gy (lower panel) were examined. Dose estimates that improved after applying the same workflow are shown on the left (labeled by original team number as outlined in Table 1), and those where dose estimates worsened are shown on the right side of the graph.

larger than the symbols. Results are summarized in the table below the graphs. The fourth column (provided material) refers to the teams' material (RNA or cDNA). Again, no. 7 refers to the reference team. Reported and re-calculated dose estimates based on *FDXR* only are shown for all three reference doses on the left side, and corresponding differences relative to the reference as well as summed absolute differences over all three reference samples (SAD) are shown on the right side. The last column provides a

comparison of the SAD for reported versus re-calculated dose estimates.

ACKNOWLEDGMENTS

We are very thankful for the technical support by Oliver Wittmann. Financial support for the Health Security Agency was provided by the National Institute for Health Research Centre for Research in Public Health Protection, UK. This work was supported by the Institute of Nuclear Chemistry and Technology statutory grant, Poland, and the Center for High-Throughput Minimally-Invasive Radiation Biodosimetry, National Institute of Allergy and Infectious Diseases Grant Number U19 AI067773.

Received: November 28, 2022; accepted: January 24, 2023; published online: April 13, 2023

REFERENCES

1. Abend M, Amundson SA, Badie C, Brzoska K, Hargitai R, Kriehuber R, et al. Inter-laboratory comparison of gene expression biodosimetry for protracted radiation exposures as part of the RENEB and EURADOS WG10 2019 exercise. Sci Rep. 2021 Dec;11(1):9756.
2. Abend M, Badie C, Quintens R, Kriehuber R, Manning G, Macaeva E, et al. Examining Radiation-Induced In Vivo and In Vitro Gene Expression Changes of the Peripheral Blood in Different Laboratories for Biodosimetry Purposes: First RENEB Gene Expression Study. Radiat Res. 2016; 185(2):109–23. DOI: 10.1667/RR14221.1
3. Barnard S, Ainsbury EA, Al-Hafidh J, Hadjidekova V, Hristova R, Lindholm C, et al. The first gamma-H2AX biodosimetry intercomparison exercise of the developing European biodosimetry network RENEB. Radiat Prot Dosimetry [Internet]. 2015 Apr 1 [cited 2022 Nov 6];164(3):265–70. Available from: https://pubmed.ncbi.nlm.nih.gov/25118318/
4. Waldner L, Bernhardsson C, Woda C, Trompier F, van Hoey O, Kulka U, et al. The 2019-2020 EURADOS WG10 and RENEB field test of retrospective dosimetry methods in a small-scale incident involving ionizing radiation. Radiat Res. 2021;195(3).
5. Endesfelder D, Oestreicher U, Kulka U, Ainsbury EA, Moquet J, Barnard S, et al. RENEB/EURADOS field exercise 2019: robust dose estimation under outdoor conditions based on the dicentric chromosome assay. Int J Radiat Biol [Internet]. 2021 [cited 2022 Nov 6];97(9):1181–98. Available from: https://pubmed.ncbi.nlm.nih.gov/34138666/
6. Gregoire E, Barquinero JF, Gruel G, Benadjaoud M, Martinez JS, Beinke C, et al. RENEB Inter-Laboratory comparison 2017: limits and pitfalls of ILCs. Int J Radiat Biol [Internet]. 2021 [cited 2022 Nov 6];97(7):888–905. Available from: https://pubmed.ncbi.nlm.nih.gov/33970757/
7. Oestreicher U, Samaga D, Ainsbury E, Antunes AC, Baeyens A, Barrios L, et al. RENEB intercomparisons applying the conventional Dicentric Chromosome Assay (DCA). Int J Radiat Biol [Internet]. 2017 Jan 2 [cited 2022 Nov 6];93(1):20–9. Available from: https://pubmed.ncbi.nlm.nih.gov/27766931/
8. Barquinero JF, Beinke C, Borràs M, Buraczewska I, Darroudi F, Gregoire E, et al. RENEB biodosimetry intercomparison analyzing translocations by FISH. Int J Radiat Biol [Internet]. 2017 Jan 2 [cited 2022 Nov 6];93(1):30–5. Available from: https://pubmed.ncbi.nlm.nih.gov/27705052/
9. Moquet J, Barnard S, Staynova A, Lindholm C, Monteiro Gil O, Martins V, et al. The second gamma-H2AX assay intercomparison exercise carried out in the framework of the European biodosimetry network (RENEB). Int J Radiat Biol. 2017;93(1).
10. Depuydt J, Baeyens A, Barnard S, Beinke C, Benedek A, Beukes P, et al. RENEB intercomparison exercises analyzing micronuclei (Cytokinesis-block Micronucleus Assay). Int J Radiat Biol [Internet]. 2017 Jan 2 [cited 2022 Nov 6];93(1):36–47. Available from: https://pubmed.ncbi.nlm.nih.gov/27673504/
11. Manning G, Macaeva E, Majewski M, Kriehuber R, Brzóska K, Abend M, et al. Comparable dose estimates of blinded whole blood samples are obtained independently of culture conditions and analytical approaches. Second RENEB gene expression study. Int J Radiat Biol. 2017;93(1).
12. Chaudhry MA. Biomarkers for human radiation exposure. J Biomed Sci. 2008 Sep;15(5):557–63.
13. Cytogenetic Dosimetry: Applications in Preparedness for and Response to Radiation Emergencies. Vienna: International Atomic Energy Agency; 2011.
14. Rothkamm K, Beinke C, Romm H, Badie C, Balagurunathan Y, Barnard S, et al. Comparison of established and emerging biodosimetry assays. Radiat Res. 2013; 180(2):111–9.
15. Amundson SA, Do KT, Shahab S, Bittner M, Meltzer P, Trent J, et al. Identification of Potential mRNA Biomarkers in Peripheral Blood Lymphocytes for Human Exposure to Ionizing Radiation. Radiat Res. 2000; 154:342-6.
16. Dressman HK, Muramoto GG, Chao NJ, Meadows S, Marshall D, Ginsburg GS, et al. Gene expression signatures that predict radiation exposure in mice and humans. PLoS Med. 2007; 4:e106. doi: 10.1371/journal.pmed.0040106
17. Badie C, Kabacik S, Balagurunathan Y, Bernard N, Brengues M, Faggioni G, et al. Laboratory intercomparison of gene expression assays. Radiat Res. 2013; 180(2):138–48.
18. Port M, Ostheim P, Majewski M, Voss T, Haupt J, Lamkowski A, et al. Rapid High-Throughput Diagnostic Triage after a Mass Radiation Exposure Event Using Early Gene Expression Changes. Radiat Res. 2019;192(2):208–18. Available from: https://pubmed.ncbi.nlm.nih.gov/31211643/
19. Paul S, Amundson SA. Development of Gene Expression Signatures for Practical Radiation Biodosimetry. Int J Radiat Oncol Biol Phys. 2008; 71:1236-1244.
20. Brengues M, Paap B, Bittner M, Amundson S, Seligmann B, Korn R, et al. Biodosimetry on small blood volume using gene expression assay. Health Phys. 2010; 98:179-85.
21. Kabacik S, Mackay A, Tamber N, Manning G, Finnon P, Paillier F, et al. Gene expression following ionising radiation: Identification of biomarkers for dose estimation and prediction of individual response. Int J Radiat Biol. 2011 Feb; 87(2):115–29.
22. Boldt S, Knops K, Kriehuber R, Wolkenhauer O. A frequency-based gene selection method to identify robust biomarkers for radiation dose prediction. Int J Radiat Biol. 2012; 88:267-76.
23. Knops K, Boldt S, Wolkenhauer O, Kriehuber R. Gene Expression in Low- and High-Dose-Irradiated Human Peripheral Blood Lymphocytes: Possible Applications for Biodosimetry. Radiat Res. 2012 Sep; 178(4):304.
24. Cruz-Garcia L, O'Brien G, Sipos B, Mayes S, Love MI, Turner DJ, et al. Generation of a Transcriptional Radiation Exposure Signature in Human Blood Using Long-Read Nanopore Sequencing. Radiat Res. 2019 Dec; 193(2):143.
25. Lloyd DC, Edwards AA, Moquet JE, Guerrero-Carbajal YC. The role of cytogenetics in early triage of radiation casualties. Appl Radiat Isot. 2000; 52:1107-12.
26. Bustin SA, Benes V, Garson JA, Hellemans J, Huggett J, Kubista M, et al. The MIQE guidelines: Minimum information for publication of quantitative real-time PCR experiments. Clin Chem. 2009; 55(4):611–22.
27. Bustin SA, Wittwer CT. MIQE: A step toward more robust and reproducible quantitative PCR. Clin Chem. 2017; 63(9):1537–8.
28. DiCarlo AL, Homer MJ, Coleman CN. United States medical preparedness for nuclear and radiological emergencies. J Radiol Prot. 2021 Dec; 41(4):1420–34.
29. Kulka U, Ainsbury L, Atkinson M, Barquinero JF, Barrios L, Beinke C, et al. Realising the European network of biodosimetry (RENEB). Radiat Prot Dosimetry. 2012; 151(4):621–5.

30. Abend M, Blakely WF, Ostheim P, Schuele S, Port M. Early molecular markers for retrospective biodosimetry and prediction of acute health effects. J Radiol Prot. 2022 Mar; 42(1):010503.

31. Cruz-Garcia L, O'Brien G, Sipos B, Mayes S, Tichý A, Sirák I, et al. In Vivo Validation of Alternative FDXR Transcripts in Human Blood in Response to Ionizing Radiation. Int J Mol Sci. 2020 Oct; 21(21):7851.

32. Manning G, Kabacik S, Finnon P, Bouffler S, Badie C. High and low dose responses of transcriptional biomarkers in ex vivo X-irradiated human blood. Int J Radiat Biol. 2013 Jul;89(7):512–22.

33. Port M, Majewski M, Herodin F, Valente M, Drouet M, Forcheron F, et al. Validating Baboon Ex Vivo and In Vivo Radiation-Related Gene Expression with Corresponding Human Data. Radiat Res. 2018 Apr; 189(4):389–98.

34. Ghandhi SA, Sima C, Weber WM, Melo DR, Rudqvist N, Morton SR, et al. Dose and Dose-Rate Effects in a Mouse Model of Internal Exposure to 137Cs. Part 1: Global Transcriptomic Responses in Blood. Radiat Res. 2021;196(5):478–90.

35. Agbenyegah S, Abend M, Atkinson MJ, Combs SE, Trott KR, Port M, et al. Impact of Inter-Individual Variance in the Expression of a Radiation-Responsive Gene Panel Used for Triage. Radiat Res. 2018 Jun; 190(3):226.

36. Port M, Schmelz HU, Stassen T, Müeller K, Stockinger M, Obermair R, et al. Correcting false gene expression measurements from degraded RNA using RTQ-PCR. Diagnostic Mol Pathol. 2007; 16(1):38–49.

37. Port M, Hérodin F, Drouet M, Valente M, Majewski M, Ostheim P, et al. Gene Expression Changes in Irradiated Baboons: A Summary and Interpretation of a Decade of Findings. Radiat Res. 2021 Mar; 195(6):501–21.